electronics

Article

SPICE-Aided Nonlinear Electrothermal Modeling of an IGBT Module

Krzysztof Górecki and Paweł Górecki *

Department of Marine Electronics, Gdynia Maritime University, Morska 81–87, 81-225 Gdynia, Poland; k.gorecki@we.umg.edu.pl
* Correspondence: p.gorecki@we.umg.edu.pl

Abstract: The paper proposes a compact electrothermal model of the IGBT module in the form of a subcircuit for SPICE. This model simultaneously takes into account electrical phenomena occurring in the module components and thermal phenomena occurring in this module. In the description of electrical phenomena, the previously formulated models of the IGBT and the diode are used, whereas the description of thermal phenomena is original. While describing thermal phenomena, self-heating in each component, mutual thermal couplings between each pair of these components, and the influence of the dissipated power on the efficiency of heat removal are taken into account. The form of the proposed model and the results of its experimental verification for the IGBT module operating under different cooling conditions are presented. The DC characteristics of the module and the characteristics of the half-bridge converter containing the considered module are presented.

Keywords: electrothermal models; IGBT modules; modeling; mutual thermal couplings; SPICE; thermal phenomena

check for updates

Citation: Górecki, K.; Górecki, P. SPICE-Aided Nonlinear Electrothermal Modeling of an IGBT Module. *Electronics* **2023**, *12*, 4588. https://doi.org/10.3390/electronics12224588

Academic Editors: Vincenzo d'Alessandro, Antonio Pio Catalano and Ciro Scognamillo

Received: 13 October 2023
Revised: 6 November 2023
Accepted: 8 November 2023
Published: 10 November 2023

1. Introduction

Power semiconductor devices are important components of DC-DC, DC-AC, and AC-DC power converters [1–3]. In order to reduce the size of the device and facilitate the assembly of these devices on the heat-sink, power modules are used which contain different semiconductor dies in the common case [1,4–6]. Such modules are manufactured in various configurations, but most often they contain transistors and diodes connected in a branch of an inverter. They contain such semiconductor devices, as power MOSFETs, diodes, or IGBTs [7–9].

As it is shown in many papers [10–15], temperature affects properties of semiconductor devices. Its increase shortens their life time [10,11] and influences the characteristics of these devices [12–15]. The junction temperature of any semiconductor device situated on the common substrate with other devices is the sum of two components. These are the ambient temperature and a temperature increase caused by thermal phenomena such as self-heating and mutual thermal couplings. Such couplings occur between the devices contained in the same case or placed on a common substrate [16–19]. The characteristics of semiconductor devices, whose every point is measured in the thermally steady state, are called non-isothermal characteristics [20], and their shape often differs significantly from the isothermal characteristics provided by manufacturers [14,21].

Non-isothermal characteristics describe the properties of semiconductor devices at the thermally steady state. In such a characteristic, each point corresponds to a different value of the junction temperature. Such a characteristic has to be measured using a point-by-point measurement method and visibly differs from the classical isothermal characteristics measured using the pulse method and presented in the datasheet. In contrast to non-isothermal characteristics, in isothermal characteristics, each point corresponds to the same value of the junction temperature equal to the ambient temperature.

In order to make the designing process of electronic networks faster and easier, some computer simulations are typically used [10,11,21,22]. Obtaining the reliable results of such simulations requires accurate models of the electronic components contained in the analyzed networks. In the description of semiconductor devices contained in power electronics, it is very important to take into account thermal phenomena. In order to perform computer analyses while taking into account these phenomena, the use of a special kind of model is indispensable. Such models are called electrothermal models. They are well-described in the literature for semiconductor devices and integrated circuits or power modules [12–14,20,23].

Compact models of power modules dedicated to network simulations are discussed, i.e., in the papers [9,24–29]. The second important group of models includes detailed models formulated, for example, using the FEM or FDM methods [30–32]. They make it possible to compute the temperature distribution in the module, but they are dedicated to single devices only and their use in network simulations is complicated [9,25]. Unfortunately, such analyses require technological data, e.g., the dimensions of individual material layers of the devices, which are not available to the users.

The paper [28] presents a compact thermal model of an IGBT module containing an IGBT and a diode. The model was formulated on the basis of the measured transient thermal impedance waveforms and verified with microscopic computations. Unfortunately, this model does not take into account mutual thermal couplings between the dies.

On the other hand, in [29], a model is proposed that takes into account the non-uniformity of temperature distribution in the module. Electrical phenomena occurring in the module are analyzed in detail, taking into account, e.g., precise determination of internal inductances of the module and differences in switching losses related to overvoltages and overcurrents. The process of determining the parameters of such a model is tedious, and its implementation requires an access to the technological data of the module.

The paper [24] is devoted to the problem of modeling mutual thermal couplings and their modeling on the basis of the material data, whereas the papers [17,33] describe compact thermal models of dies placed on a common substrate. The thermal models presented in [9,25–33] are characterized by a simplified description of the electrical properties of the modeled device. This means that when using such kinds of models, the operating point is not accurately computed and the device junction temperature can be computed only at the known values of the dissipated power.

The paper [34] shows the results of measurements of nonisothermal characteristics of a selected IGBT module and the first version of an electrothermal model of such an IGBT module. The shape of these characteristics visibly changes due to self-heating and mutual thermal couplings. This model makes it possible to compute only the DC characteristics and its verification is performed in one type of cooling condition only. The cited paper proves that proper modeling of IGBTs in the sub-threshold region is very important.

In the paper [33], it is shown that self and transfer thermal resistances in the IGBT module depend on the power dissipated in this module. The junction temperatures of the module components may significantly differ from each other.

In this paper, a new electrothermal model of the IGBT module dedicated for the SPICE software is proposed. It simultaneously takes into account electrical phenomena in the components of the module and thermal phenomena occurring in this module. The description of the electrical phenomena is based on the electrical models of an IGBT and a diode published previously in [15,17,21], whereas the description of the thermal model is original. Self-heating in each component, mutual thermal couplings between each pair of these components, and the influence of the dissipated power on the efficiency of heat removal are taken into account. The detailed considerations are carried out for the module containing two IGBTs, two diodes, and a thermistor. The experimental verification of the correctness of the proposed model was performed both for the DC and transient analyses. The obtained results of measurements and computations of the DC characteristics of the components of the module and the characteristics of the half-bridge converter with the considered module are presented and discussed.

2. Model Form

The elaborated model describes properties of a typical IGBT module containing IGBTs and p-i-n diodes connected to the inverter branch and a thermistor as shown in Figure 1.

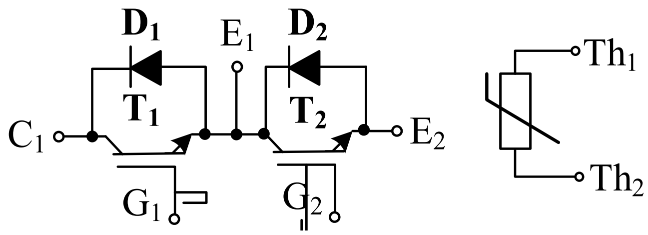

Figure 1. Internal connections of the components of the tested IGBT module.

This module has two control leads (G_1 and G_2), three high-current leads (C_1, E_1, and E_2), and two thermistor leads (Th_1 and Th_2) to monitor the temperature of the module base. Both the IGBTs and the diodes are electrically connected one to another, whereas the thermistor is not connected electrically to the mentioned devices. Only thermal couplings occur between these IGBTs, diodes, and the thermistor.

The formulated electrothermal model of the IGBT module belongs to the group of compact electrothermal models and takes into account electrical and thermal phenomena occurring in each component and between them. It makes it possible to determine voltages and currents of all the components of the considered IGBT module and their junction temperatures. The block structure of the proposed model is shown in Figure 2.

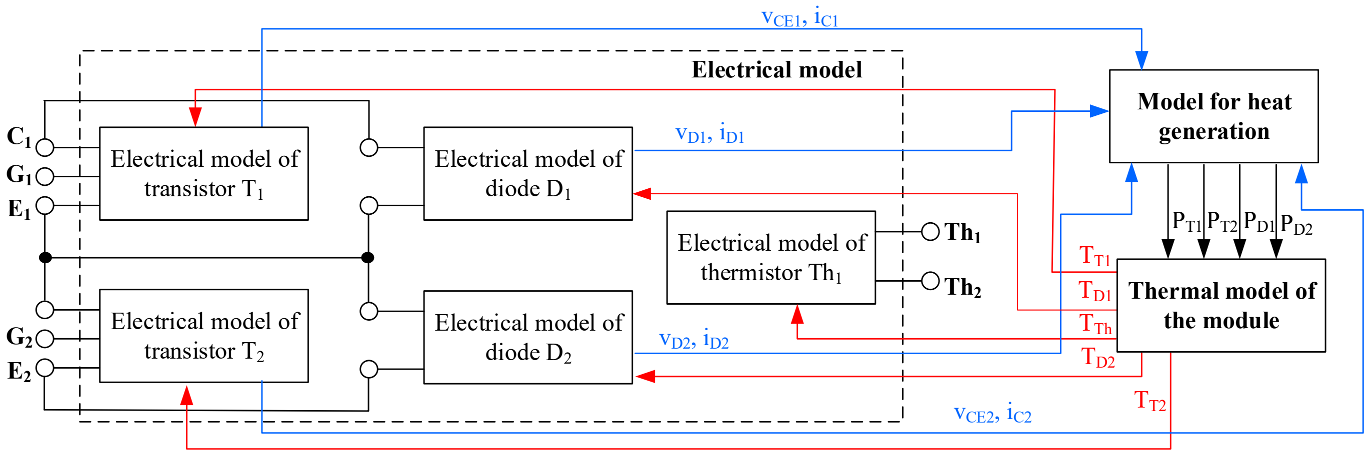

Figure 2. Block diagram of the electrothermal model of the tested IGBT module.

There are three blocks in this model: an electrical model, a model for heat generation, and a thermal model of the module. The electrical model describes the dependences between currents and voltages of the modeled device, taking into account the influence of its junction temperature. The terminals of this model (G_1, G_2, C_1, E_1, and E_2) correspond to the terminals of the actual module. The thermal model describes the dependence of the junction temperature of each component on the power dissipated in this component and in the other components contained in the module. Voltages on the terminals of this model correspond to the junction temperature of transistors (T_{T1} and T_{T2}), diodes (T_{D1} and T_{D2}), and the thermistor (T_{th}). The model for heat generation contains dependences of the power dissipated in each of the modeled components on their voltages and currents. These powers correspond to voltages on terminals P_{T1} and P_{T2} (for transistors), P_{D1}, and P_{D2} (for diodes). The power dissipated in the thermistor is so low that it can be omitted and its value is not computed in the model.

The parts of this models are described in Section 2.1 (electrical model), Section 2.2 (model for heat generation), and Section 2.3 (thermal model), whereas the method of the model parameter estimation is described in Section 2.4.

2.1. Electrical Model

The electrical model of the module consists of electrical models of all the components of this module. These models are connected according to the diagram shown in Figure 1. Both IGBTs (T_1 and T_2) are described by the same models, similarly as both the diodes (D_1 and D_2). The used electrical model of the IGBT is described in the papers [15,21] and its schematic diagram is given in Figure 3a. In this model, the following phenomena are taken into account:

(a) DC properties of the output bipolar structure and the input MOS structure including the sub-threshold effect and the dependence of the threshold voltage on its junction temperature, the dependence of the current amplification factor of the BJT structure on the collector current and temperature, and leakage currents (DC model of the IGBT);

(b) Series resistance of emitter R_E and collector R_C modeled by linear resistors, the resistance of which linearly depends on the transistor junction temperature;

(c) The dependence of the capacitance between each pair of the leads of the IGBT on voltage and the junction temperature represented by the controlled current sources G_{CGE}, G_{CCE}, and G_{CGC}.

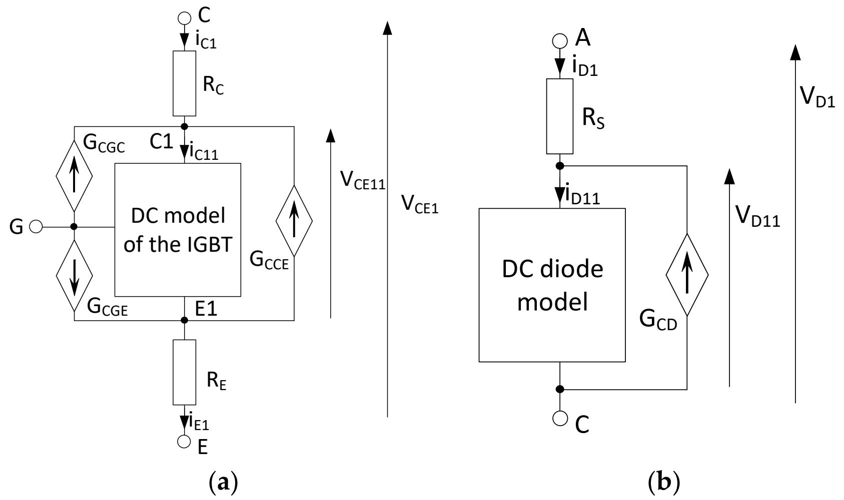

Figure 3. Diagrams of electrical models of: the IGBT (**a**) and the diode (**b**).

The equations describing the electrical model of the IGBT used in the described electrothermal model of the IGBT module are given in [15]. In this model, both the dependences describing I-V and C-V characteristics occur. An influence of the junction temperature of these characteristics is taken into account. While formulating behavioral dependences describing the influence of temperature on the C-V, the characteristics waveforms of the collector current of the transistor operating as a switch with resistance load measured at different values of temperature are used. Such characteristics are presented in the paper [21].

In turn, the electrical model of the diode, the diagram of which is shown in Figure 3b, takes into account the following:

- the diffusion and generation-recombination components of the current of this component (DC diode model), described using the same equation as for the power LED presented, i.e., in [17];
- the linear dependence of the diode series resistance on its junction temperature;

- a nonlinear capacitance of the p-n junction depending on the junction voltage and temperature represented by the current source G_{CD}.

The DC model of the diode is represented by the single controlled current source. This source describes the dependence of diffusion and generation-recombination components of the DC diode current on voltage v_{D11} marked in Figure 3b.

In turn, the DC model of the IGBT (occurring in Figure 3a) has a network representation shown in Figure 4.

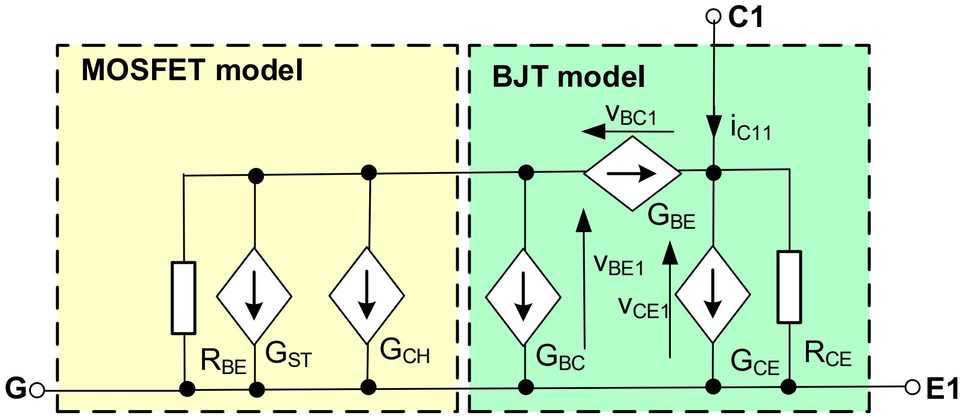

Figure 4. Network representation of the DC model of the IGBT.

The classical network representation of the IGBT is used in the form of connection of the input MOSFET structure and the output BJT. In the presented model, resistors R_{CE} and R_{BE} model the leakage currents of the modeled device. The drain current of the MOSFET structure is modeled by two controlled current sources: G_{ST} and G_{CH}. The first of these sources describes the drain current in the sub-threshold region. The source G_D describes the MOSFET channel current.

Current flowing between the base and the emitter of the BJT is modeled by the controlled current source G_{BE}. The controlled current source G_{BC} models the current flowing between the base and the collector of the BJT. The main current of the IGBT is modeled by the controlled current source G_{CE}. All the equations describing the mentioned current sources are given in the paper [15].

The electrical model of the thermistor contains the controlled current source of the output current given by the equation of the form:

$$i_{th} = \frac{V_{th}}{R_0} \cdot \exp\left(\frac{B}{T_0} - \frac{B}{T_{th}}\right) \tag{1}$$

where R_0 denotes the resistance of this component in the reference temperature T_0, B is a thermistor parameter describing the slope of the dependence of the thermistor resistance on temperature T_{th}, and V_{th} is voltage on the thermistor.

2.2. Model for Heat Generation

The model for heat generation is used to compute values (in the DC analysis) or waveforms (in the transient analysis) of the active power dissipated in each of the module component. The power dissipated in each transistor is given by the same equation, which for transistor T_1 has the following form:

$$p_{T1} = i_{C11} \cdot v_{CE11} + R_C \cdot i_{C1}^2 + R_E \cdot i_{E1}^2 \tag{2}$$

where currents i_{C1}, i_{E1}, and voltage V_{CE1} are marked in Figure 3a.

For each diode the same equation describes the active power dissipated in it. It has the following form for diode D_1:

$$p_{D1} = i_{D11} \cdot v_{D11} + R_S \cdot i_{D1}^2 \tag{3}$$

where currents i_{D1}, i_{D11}, and voltage v_{D11} are marked in Figure 3b.

2.3. Thermal Model

The thermal model of the module is used to compute the waveforms of the junction temperature of each component of the module, taking into account self-heating in each component and mutual thermal couplings between each pair of these components. Temperatures of these components are given by the equations of the same form, which for transistor T_1 is as follows:

$$\begin{gathered} T_{T1}(t) = T_a + \int_0^t p_{T1}(v) \cdot Z'_{thT1}(t-v)dv + \int_0^t p_{T2}(v) \cdot Z'_{thT1T2}(t-v)dv + \\ + \int_0^t p_{D1}(v) \cdot Z'_{thT1D1}(t-v)dv + \int_0^t p_{D2}(v) \cdot Z'_{thT1D2}(t-v)dv \end{gathered} \tag{4}$$

where $p_{T1}(t)$, $p_{T2}(t)$, $p_{D1}(t)$, and $p_{D2}(t)$ denote the waveforms of the powers dissipated in T_1 and T_2 transistors and in D_1 and D_2 diodes, respectively. $Z'_{thT1}(t)$ is a time derivative of self-transient thermal impedance of transistor T_1, whereas $Z'_{thT1T2}(t)$, $Z'_{thT1D1}(t)$, and $Z'_{thT1D2}(t)$ denote time derivatives of transfer transient thermal impedances between transistor T_1 and each of the other components of the investigated module (transistor T_2, diodes D_1 and D_2), respectively.

Both the self and transfer transient thermal impedances $Z_{thk}(t)$ are described with the equation of the form [35]:

$$Z_{thk}(t) = R_{thk} \cdot \left[1 - \sum_{i=1}^{N_k} a_{ki} \cdot \exp\left(-\frac{t}{\tau_{thki}}\right)\right] \tag{5}$$

where R_{thk} is thermal resistance, a_{ki} denotes the coefficient corresponding to the thermal time constant τ_{thki}, and N_k is the number of thermal time constants. The parameters occurring in Equation (5) depend on the cooling system used. Additionally, as it is shown in [35], the value of thermal resistance is a decreasing function of the dissipated power. In the proposed model, this dependence is described as follows:

$$R_{thk} = R_{thk0} \cdot [1 + c_k \cdot \exp(-p/b_k)] \tag{6}$$

where R_{thk0} denotes the minimum value of R_{thk}, p is the power dissipated in the heat source, whereas c_k and b_k are parameters, the values of which depend on the cooling conditions. The Equation (6) is used to describe each of self and transfer thermal resistances.

In the SPICE software, the network representation of each of the equations used in the model are needed. The network representation of the Equation (4) is shown in Figure 5. It makes it possible to compute temperature T_{T1} using the subcircuit denoted with the letter A.

Each of the subcircuits visible in Figure 5 (denoted with letters B, C, and D) describes one component of the mentioned equation denoted as voltages in the nodes T_{T1T2} (subcircuit B), T_{T1D1} (subcircuit C), and T_{T1D2} (subcircuit D). These voltages represent an increase in the junction temperature of transistor T_1 caused by mutual thermal coupling between this transistor and transistor T_2, and diodes D_1 and D_2, respectively. Subcircuit A consists of three parts. The first of them, voltage source V_{Ta}, models the ambient temperature T_a. The second part, the controlled voltage source E_1, models the influence of mutual thermal couplings on the junction temperature of transistor T_1. The voltage on this source is equal to the sum of voltages in nodes T_{T1T2}, T_{T1D1}, and T_{T1D2} (Subcircuits B, C and D). The third part of this network models an increase in temperature T_{T1} caused by self-heating in this transistor.

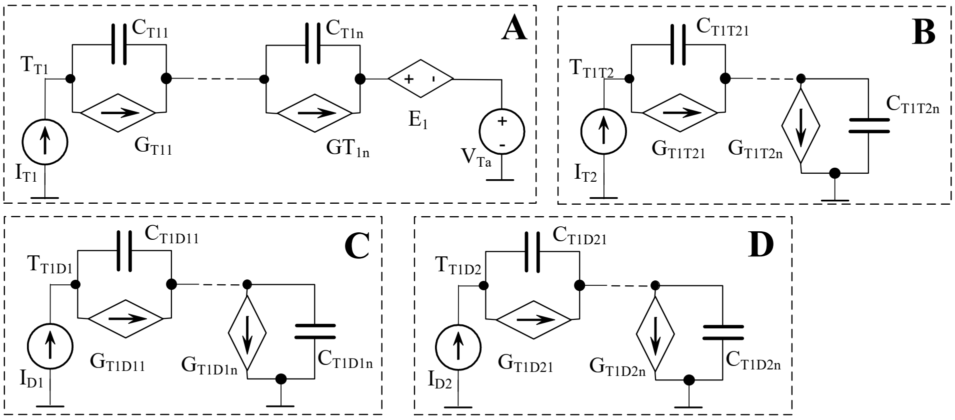

Figure 5. Network representation of Equation (4) dedicated to compute the junction temperature of transistor T_1.

In these subcircuits, current sources I_{T1}, I_{T2}, I_{D1}, and I_{D2} model the power dissipated in transistors T_1 and T_2 and diodes D_1 and D_2, respectively. The controlled current sources represent the dependences of the adequate part of self or transfer thermal resistance on the power dissipated in transistor T_1, whereas capacitors represent thermal capacitances occurring in self and transfer transient thermal impedances. The current of these sources is given by the formula of the form:

$$G_{T1ki} = \frac{V_{GT1ki}}{R_{thT1k} \cdot a_{ki}} \tag{7}$$

where V_{GT1ki} denotes voltage on the considered current source, and R_{thT1k} is the self or transfer thermal resistance modeled in the considered block of the presented network. Capacitors C_{T1ki} represent thermal capacitance described by:

$$C_{T1ki} = \tau_{thki}/R_{thk0} \tag{8}$$

The same networks as presented in Figure 5 are used also to compute the junction temperatures of transistor T_2, both the diodes and the thermistor. For the thermistor, all the subcircuits represent transfer transient thermal impedances between the thermistor and the other components of the module.

In the thermal model, the values of the parameters characterizing self-transient thermal impedances for both the transistors are identical, and the parameters for both the diodes are identical. The parameters describing the mutual thermal couplings between each pair of the module components also have the identical values, e.g., transfer thermal resistances $R_{thT1D2} = R_{thD2T1}$.

2.4. Model Parameter Estimation

There are two groups of parameters in the presented model:

- electrical parameters describing I-V and C-V characteristics of the module components;
- thermal parameters describing the dependence of the junction temperature of each module component on the power lost in these components.

The presented model does not use any technological parameters as, e.g., doping concentration. All the parameters describing the electrical properties of the IGBT and the diode can be estimated on the basis of electrical characteristics of these devices given by the manufacturers in the datasheet or some measurements performed by the user.

The values of electrical parameters are determined by the local estimation method [35], i.e., by selecting groups of parameters ensuring a good compliance of a specific fragment of the calculated and measured characteristics. The input data for the electrical parameter estimation procedure are the isothermal I-V and C-V characteristics of the diodes and transistors contained in the modeled module, measured at two ambient temperatures equal to about 25 °C and about 100 °C. This data can also come from the module's datasheet. The parameters describing the thermistor model are given by the manufacturer in the datasheet.

In turn, determining the value of thermal parameters requires the performance of measurements of self-transient thermal impedances of one diode and one transistor, and of the transfer transient thermal impedances between both the transistors, between both the diodes, between the transistor and the diode, between the transistor and the thermistor, and between the diode and the thermistor. The measurements should be made using the indirect electrical method described in [33] in a wide range of changes in the power lost in the module components. For each of the measured waveforms of self and transfer transient thermal impedances, values of the parameters appearing in the Equation (5) should be determined using the method described in [35].

The parameters appearing in Equation (6) are determined by approximating the measured dependences of self and transfer thermal resistances R_{thk} in the module on the power. The values of thermal parameters should be determined separately for each of the analyzed cooling systems of the modeled module.

First, the measurements of each thermal resistance for selected power values must be carried out. With the measured dependence $R_{thk}(p)$, the minimum value of this function R_{thk0} is determined, and then values of parameters c_k and b_k are determined by the least squares method with regard to the linear function of the form:

$$\ln(R_{thk}/R_{thk0} - 1) = -p/b_k + \ln(c_k) \tag{9}$$

3. Investigations Results

Using the proposed model of the IGBT module, some characteristics of such a module are computed and compared with the measurement results. The investigations were performed for the IGBT module of the type PSI25/06 (PowerSem GmbH, Walpersdorfer, Germany). In Section 3.1, the most important parameters of this module are given. Section 3.2 presents the measured and computed DC characteristics of the module operating at different cooling conditions, whereas in Section 3.3, the measured and computed characteristics of the half-bridge converter including the considered module are given. In all the figures given in Sections 3.2 and 3.3, the points denote the results of measurements, whereas lines denote the results of computations.

3.1. Investigated Module

The investigated power module includes IGBTs, diodes, and a thermistor [36]. These IGBTs are characterized by: the maximum collector-emitter voltage V_{CES} = 600 V, the maximum continuous collector current at room temperature I_{C25} = 24.5 A, and the thermal resistance between the chip and the case which amounts to 1.52 K/W [36].

The maximum continuous forward current of the diodes is equal to 18.5 A, and thermal resistance between the junction and the case is equal to 3 K/W [36]. The thermistor parameters are as follows: R_0 = 5 kΩ, T_0 = 298 K, and B = 3375 K.

3.2. DC Module Characteristics

In order to illustrate the influence of the ambient temperature on the DC characteristics of the tested module, Figures 6 and 7 show the isothermal characteristics of diode D_2 (Figure 6) and the transfer characteristics of transistor T_1 (Figure 7). The presented measurement results are obtained using the pulse method and the Keithley (Cleveland, OH, USA) 2612 sourcemeter.

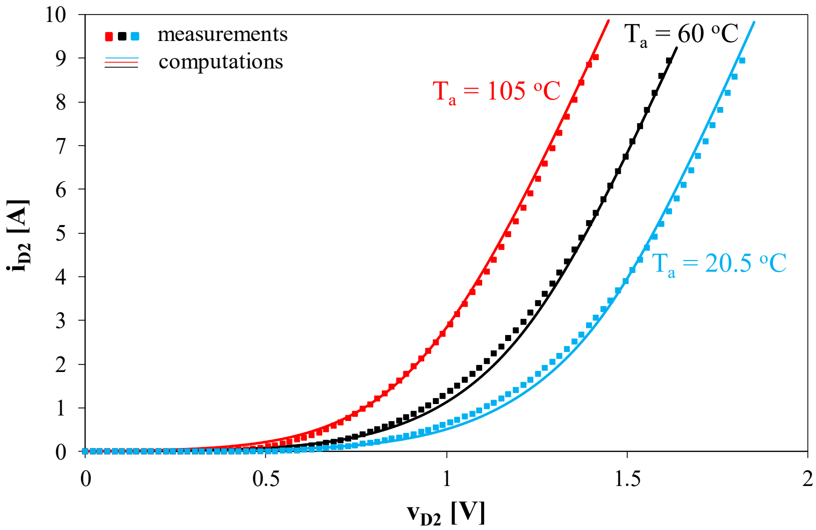

Figure 6. Measured and computed isothermal characteristics of diode D_2.

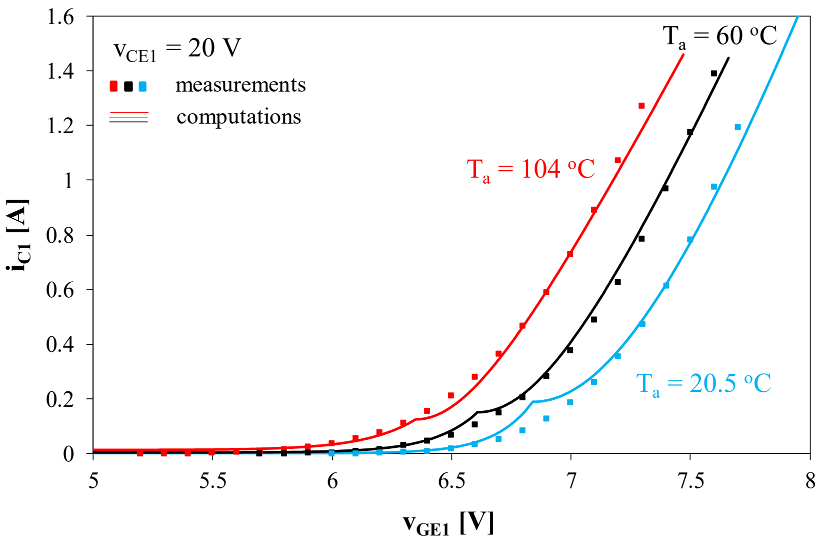

Figure 7. Measured and computed isothermal transfer characteristics of transistor T_1.

As it is visible, an increase in the ambient temperature causes the diode forward voltage to drop over a wide range of the diode forward current. In the range of high current values, the characteristics determined for different T_a values are practically parallel. This means that the series resistance of the diode is practically independent of temperature. Additionally, it can be seen that the temperature coefficient of the forward voltage exceeds -5 mV/°C, which is a much higher value than for the classic p-n diodes.

In Figure 7, it is visible that an increase in temperature causes the transfer characteristic to be shifted to the left due to the negative temperature coefficient of change in the threshold voltage. At room temperature, it amounts to 6.8 V. A sub-threshold effect is visible on the presented characteristics, which causes the collector current to increase at voltage V_{GE1} lower than the threshold voltage. It is also visible that for the curves obtained from the computations, non-smooth points occur. These points are the result of the use a spline in the description of the current flowing through the input MOS structure of the IGBT. Such points are visible at the border between the sub-threshold and saturation regions of operation of these structure.

Figures 8–13 present non-isothermal (solid lines) characteristics of the components of the tested module. In these figures, dashed lines mark the isothermal characteristics of the tested transistor. In addition to the current-voltage dependences, there are also dependences of the module case temperature T_C equal to the thermistor temperature T_{Th} on selected voltages on its terminals. The tests are carried out for a module without a heat-sink and a module placed on a heat-sink of the dimensions 60 × 140 mm with 11 fins 30 mm high.

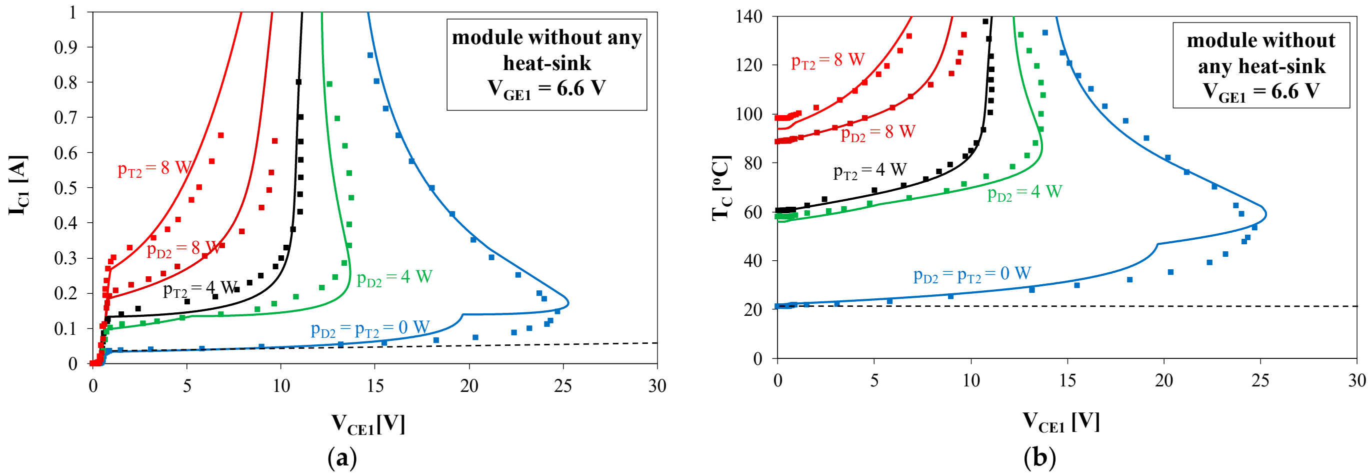

Figure 8. Computed and measured nonisothermal output characteristics of transistor T_1 at V_{GE1} = 6.6 V (**a**) and dependences of temperature T_C on V_{CE1} voltage (**b**) at different values of the power dissipated in the other components of the module operating without any heat-sink.

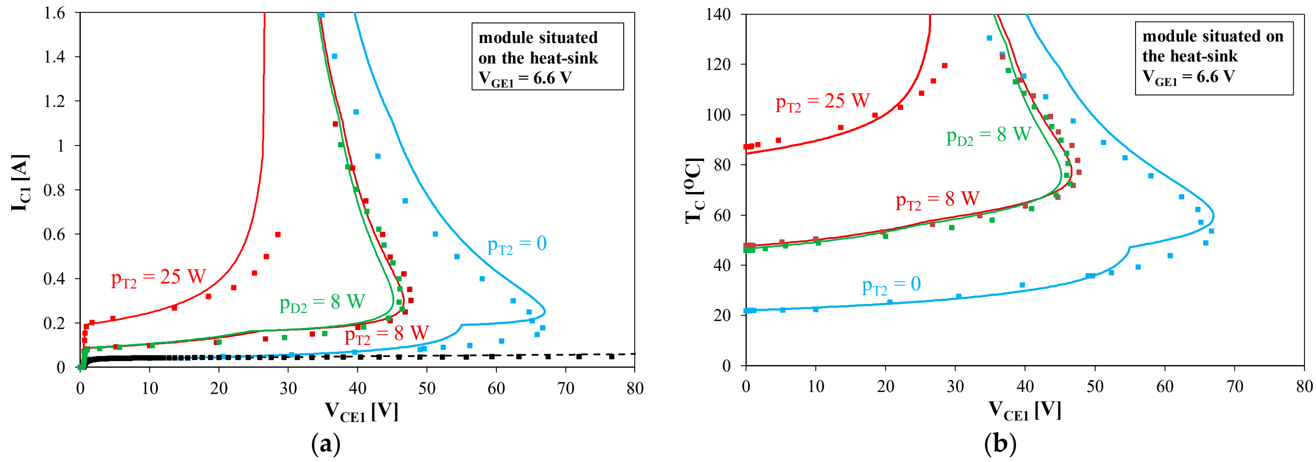

Figure 9. Computed and measured output characteristics of transistor T_1 at V_{GE1} = 6.6 V (**a**) and dependences of temperature T_C on V_{CE1} voltage (**b**) at different values of the power dissipated in the other components of the module situated on the heat-sink.

In the computations, the measured values of the parameters characterizing the properties of the heat removal system in the steady state, given in Table 1, are used.

The measurements of non-isothermal characteristics were carried out with the use of power supplies Keithley 2260B-30-36, Keithley 2260B-250-4, and laboratory multimeters Rigol DM3068. All the results presented in Figures 8–13 were determined at the thermally steady state using the measurement systems shown in [31]. The measured isothermal characteristics were obtained using the pulse method and the Keithley 2612 sourcemeter.

For the transistor, the output characteristics were measured and computed at voltage V_{GE} = 6.6 V, which slightly exceeds the threshold voltage of the transistor and at V_{GE} = 15 V, which significantly exceeds the threshold voltage.

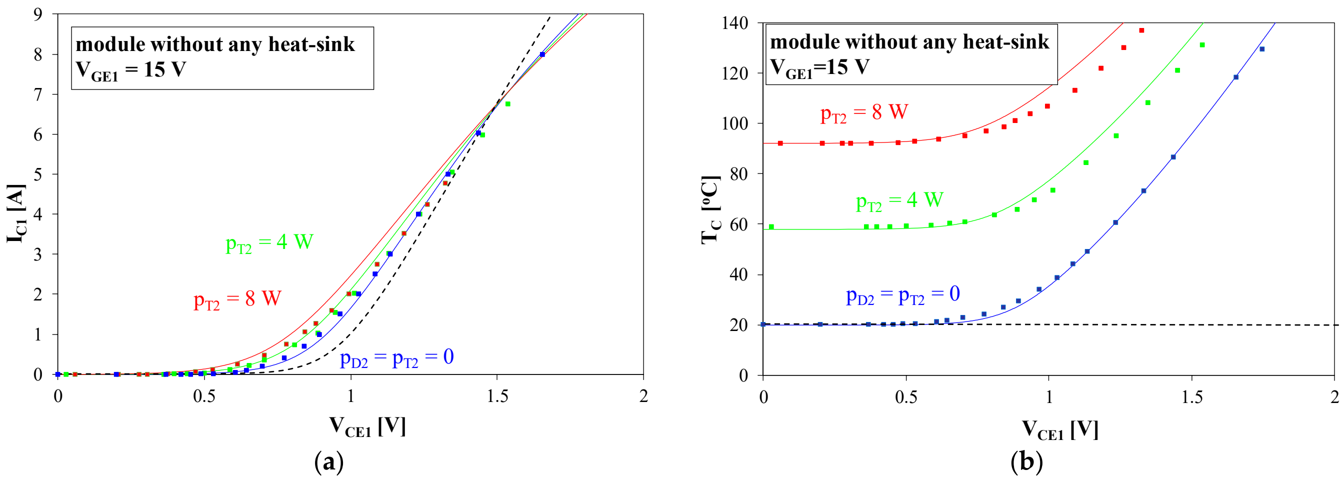

Figure 10. Computed and measured nonisothermal output characteristics of transistor T_1 at V_{GE1} = 15 V (**a**) and dependences of temperature T_C on V_{CE1} voltage (**b**) at different values of the power dissipated in the other components of the module operating without any heat-sink.

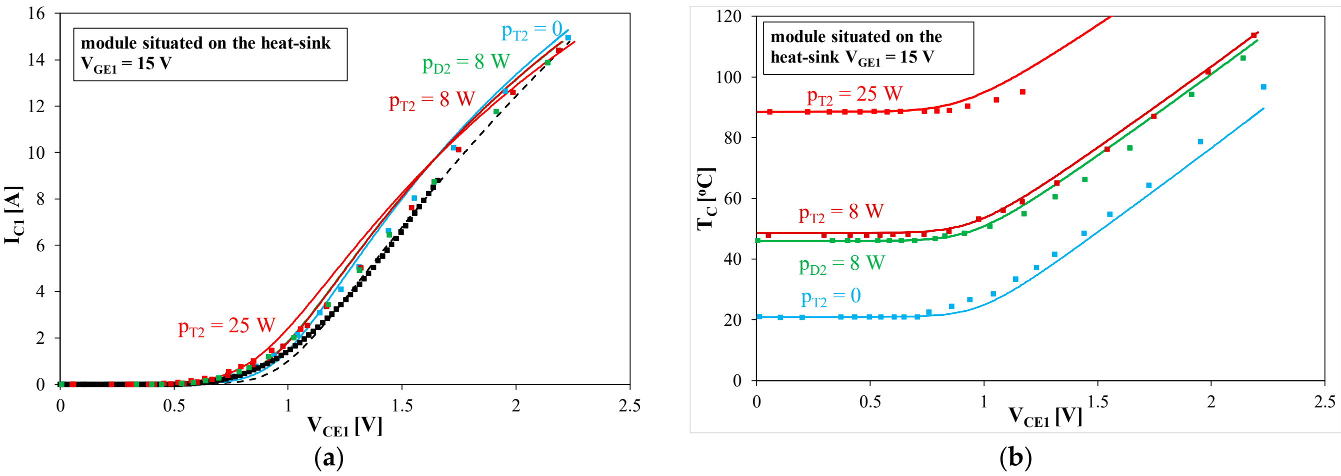

Figure 11. Computed and measured output characteristics of transistor T_1 at V_{GE1} = 15 V (**a**) and dependences of temperature T_C on V_{CE1} voltage (**b**) at different values of the power dissipated in the other components of the module situated on the heat-sink.

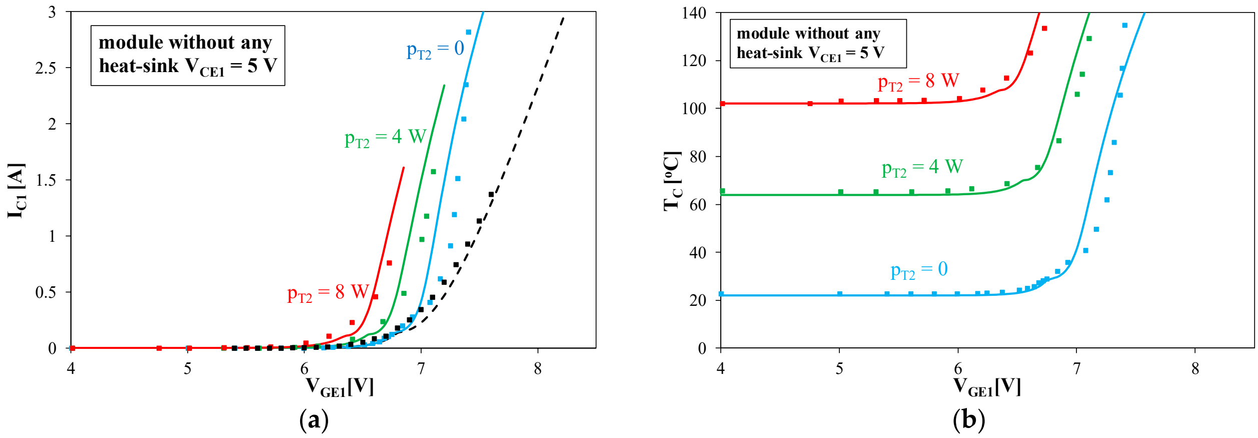

Figure 12. Computed and measured nonisothermal transfer characteristics of transistor T_1 at V_{CE1} = 5 V (**a**) and dependences of temperature T_C on V_{GE1} voltage (**b**) and different values of the power dissipated in the other components of the module operating without any heat-sink.

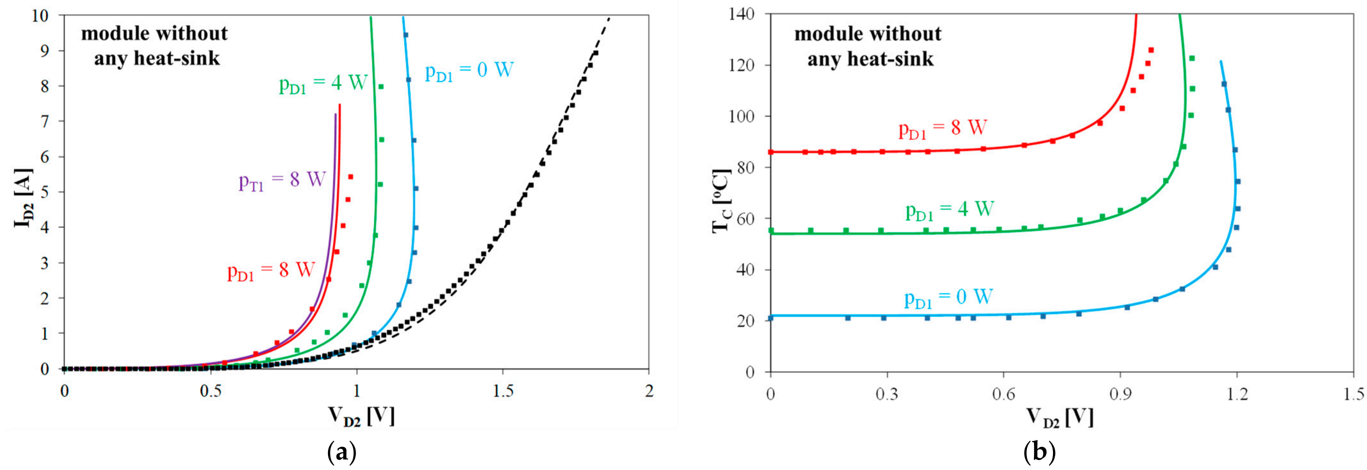

Figure 13. Computed and measured characteristics of diode D_2 (**a**) and dependences of temperature T_C on V_{D2} voltage (**b**) at different values of the power dissipated in diode D_1 or in transistor T_1 for the module operating without any heat-sink.

Table 1. Parameters values describing thermal resistances in the IGBT module model.

Parameter	Module without Any Heat-Sink			Module on the Heat-Sink		
	R_{thk0} [K/W]	c_k	b_k [W]	R_{thk0} [K/W]	c_k	b_k [W]
$R_{thT1} = R_{thT2}$	11.5	0.522	3.8	2.5	0.88	20
$R_{thD1} = R_{thD2}$	12	0.5	3.8	4	0.55	20
R_{thT1T2}	11.5	0.53	3.8	2.4	0.56	15
$R_{thT1D1} = R_{thT2D2}$	8	0.48	3.8	2.6	0.58	15
R_{thD1D2}	8.5	0.45	3.8	3	0.4	15
$R_{thT1D2} = R_{thT2D1}$	8	0.48	3.8	2.6	0.55	15
$R_{thT1Th} = R_{thT2Th}$	7.5	0.4	3.8	1.9	0.526	15
$R_{thD1Th} = R_{thD2Th}$	8.5	0.353	3.8	2	0.5	15

In Figure 8a, the output characteristics of transistor T_1 at V_{GE1} = 6.6 V are shown for the module operating without any heat-sink, whereas Figure 8b shows the corresponding dependences of temperature T_C on the collector-emitter voltage of transistor T_1. The investigations were performed at different values of the power dissipated in the other components of the module (power p_{D2} in diode D_2 and power p_{T2} in transistor T_2).

As it is visible, the shape of the presented nonisothermal characteristics differs significantly from the isothermal ones. They are not any mathematical functions. Any point of an electrothermal breakdown is visible on each of them. In such a point a sign of the slope of these characteristics changes. The value of voltage V_{CE1}, at which such a point appears decreases if the power dissipated in the other components of the module increases. Due to thermal phenomena, the value of the collector current increases when this power increases. It is worth noticing that the dissipation of the power in transistor T_2 causes a stronger influence on the course of the characteristic $I_{C1}(V_{CE1})$ than the dissipation of the power of the same value in diode D_2. Additionally, it is visible in Figure 8b that the changes in the shape of characteristics $I_{C1}(V_{CE1})$ are accompanied by the essential changes in temperature T_C. Due to mutual thermal couplings between the components of the module, a rise in T_C temperature exceeds even 100 °C.

As can be seen in Figure 9, the shape of the dependence $I_{C1}(V_{CE1})$ obtained for the module placed on the heat-sink is similar to that for the module operating without any heat-sink. It is worth noting that the electrothermal breakdown point occurs at higher voltage V_{CE1} than for a module without a heat-sink. The change in the value of this voltage can be even sevenfold (with p_{T2} = 8 W). With the considered cooling conditions, the influence of the selection of the component, in which the power is dissipated, is hardly visible on the characteristics of transistor T_1. This is due to a lower temperature rise inside the transistor caused by mutual thermal couplings. For comparison, it is worth noting that under the isothermal conditions, a practically constant value of the collector current of only 50 mA is obtained (black points and lines).

In Figures 8a and 9a, an increase in the collector current is visible due to mutual thermal couplings and an increase in the junction temperature of the transistor. In turn, in Figure 8b, it can be seen that at the electrothermal breakdown point, the junction temperature increase in the transistor above the sum of the ambient temperature and its increase caused by mutual thermal coupling is only 30 °C. Due to the more effective heat removal, the point of the electrothermal breakdown is observed at a higher value of voltage V_{CE1} for the module mounted on the heat-sink than for the module operating without any heat-sink. Similarly as in Figure 7, in Figures 8 and 9, one can observe non-smooth points near the border between the sub-threshold and saturation region of operation of the input MOS structure of the IGBT.

In turn, Figure 10 illustrates the influence of thermal phenomena on the output characteristics of transistor T_1 (Figure 10a) and on the dependence of the thermistor temperature on V_{CE1} voltage at V_{GE1} = 15 V. In such operating conditions, thermal phenomena slowly influence the courses of the output transistor characteristics visible mostly at current $I_{C1} \leq 4$ A. On the other hand, a strong influence of thermal phenomena on temperature T_C is observed. This temperature exceeds even 140 °C. The mutual thermal couplings cause a decrease in the value of the maximum allowable current I_{C1} from 8 A when the power is dissipated only in transistor T_1 to 5 A when the power p_{T2} = 8 W is dissipated in transistor T_2.

In Figure 11, it can be seen that thermal phenomena cause the voltage value V_{CE1} to drop for currents $I_{C1} < 10$ A. For higher values of this current, voltage V_{CE1} increases with an increase in the power dissipated in the components of the IGBT module. When the power dissipated in the other transistor is 25 W, the maximum value of the collector current I_{C1} is only 20% of the value of this current obtained when no power was dissipated in the other components of the investigated module.

Figure 12 illustrates the transfer characteristics of transistor T_1 for the module without any heat-sink.

As can be seen, due to thermal phenomena, the transfer characteristics of the transistor under consideration shift to the left. The course of these characteristics in the range of voltage V_{GE} higher than the threshold voltage is very steep. Mutual thermal couplings cause an increase in the module temperature by up to 80 °C, which, with current I_{C1} = 1 A, translates into a voltage drop of V_{GE1} even by 0.4 V.

Figure 13 illustrates the isothermal and non-isothermal characteristics of diode D_2 contained in the module operating without any heat-sink.

As it is visible, an increase in the power dissipated in the module causes the characteristics to shift to the left. The presented non-isothermal characteristics show an electrothermal breakdown point, which proves that this diode is characterized by a very low series resistance value. It is worth noting that at high current values, a decrease in the forward voltage caused by self-heating is even 0.7 V. Due to the power dissipation of 8 W in diode D_1 or in transistor T_1, the allowable value of the diode D_2 current decreases twice. It is visible that the influence of mutual thermal couplings on the considered characteristics very weakly depends on the location of the heat source, and the characteristics obtained at the dissipation power equal to 8 W in diode D_1 and in transistor T_1 are nearly the same. Qualitatively the identical characteristics are obtained for the module situated on a heat-sink.

Comparing the results of the computations and measurements presented in this section, it can be seen that the proposed model enables the correct computation of both the isothermal and non-isothermal characteristics of all the components of the considered module. A very good agreement between the measurement and computation results is obtained both in the case of the operation of a single component of this module and the simultaneous operation of many components.

3.3. Characteristics of the Half-Bridge Converter with an IGBT Module

In order to verify the usefulness of the described model in switched-mode converters, computations and measurements of the characteristics of the classical half-bridge converter containing the considered module were carried out. The diagram of the analyzed converter is shown in Figure 14.

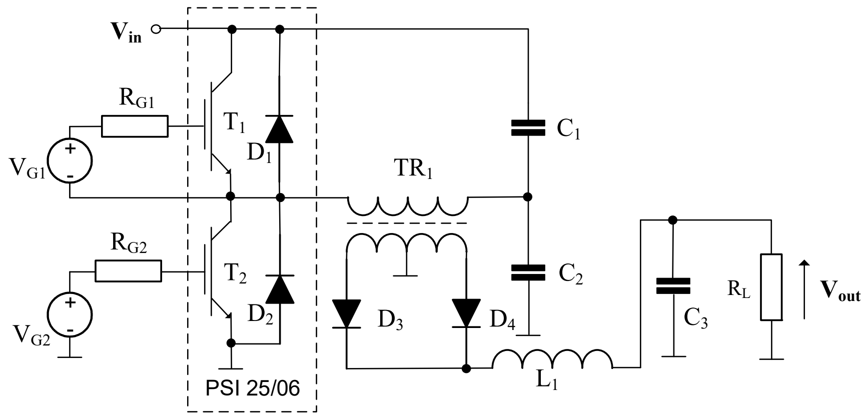

Figure 14. Diagram of the investigated half-bridge DC-DC converter.

In the considered converter, apart from the PSI 25/06 module, capacitors C_1 and C_2 with the capacitance of 680 µF and C_3 with the capacitance of 1 mF, inductor L_1 with the nominal inductance of 1 mH and series resistance 45 mΩ, a transformer TR_1 with the 2:1:1 turn ratio, and diodes D_3 and D_4 of the IDP15E60 type in TO-220 cases situated on small heat-sinks are used. The control signals are obtained from the IR2110 driver [37] represented in the diagram by voltage sources V_{G1} and V_{G2} generating rectangular pulses trains of the value of 15 V in the high state and zero in the low state. Both these signals have the same frequency f and duty cycle d, but they are shifted by half of the period in relation to each other. The resistors R_{G1} and R_{G2} are selected to be equal to 100 Ω to reduce the influence of parasitic elements on switching performance of the tested IGBT module. Values of passive components and parameters of the control signal are selected in such a way as to obtain the operation in CCM in the whole range of change in the output current. Voltage source V_{in} represents the input voltage, whereas resistor R_L is the load of the converter.

During the design of this converter, particular attention was paid to limiting the influence of parasitic effects on the operation of the IGBT module. Therefore, the length of the main lead between the V_{in} power supply and transistor T_1 was shortened to only 3 cm. As a result, the inductance of this lead is below 20 nH. This, in combination with the relatively low value of the time derivative of current I_C when switching off the transistor, resulted in the overvoltage amplitude on the module not exceeding 10 V. For this reason, the inductance of leads is omitted in the analysis.

In order to compute non-isothermal characteristics of the considered DC-DC converter at the steady-state, the method of the electrothermal transient analysis with one non-physical thermal time constant [34] is applied. In the analyses, the electrothermal model of the IGBT module described in the previous section and the electrothermal model of diodes D_3 and D_4 are used passive elements are modeled with the use of the linear models built-in in SPICE [38]. For magnetic components (transformer TR_1 and inductor L_1 together with the inductors representing inductance of each winding), the resistors representing series resistance of the windings of these components are added.

Figures 15–17 show selected characteristics of the considered converter determined at the input voltage V_{in} = 48 V, frequency f = 25 kHz, and the duty cycle d = 0.47 (red lines and points) and at V_{in} = 150 V, f = 20 kHz, and d = 0.47 (blue lines and points). Energy efficiency η of the converter is measured and computed using the average values of its output and input powers. The value of this efficiency is limited, e.g., by power losses in transistor switches. Figure 17 illustrates the computed dependence of the average value of the power losses in transistor T_1 on the converter output current.

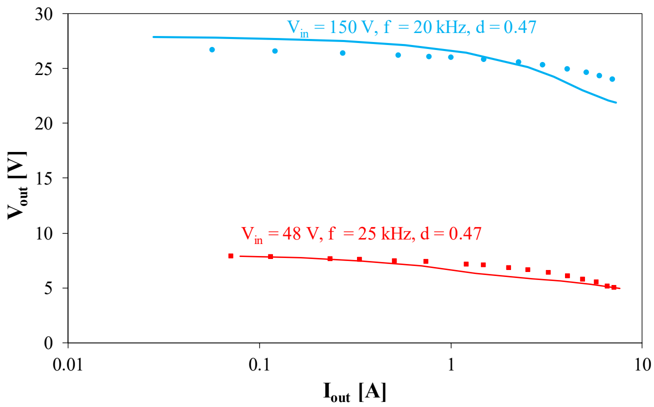

Figure 15. Computed and measured non-isothermal output characteristics of the half-bridge converter.

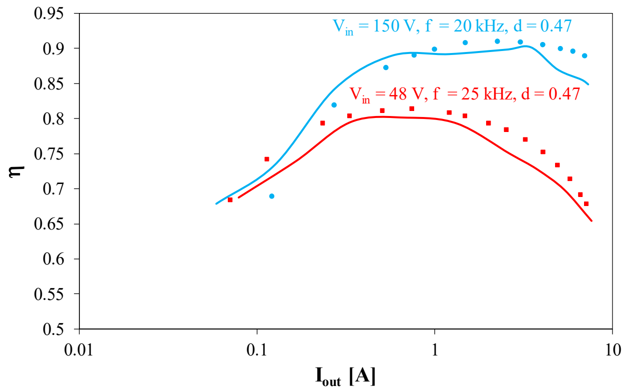

Figure 16. Computed and measured non-isothermal dependences of energy efficiency on the output current of the half-bridge converter.

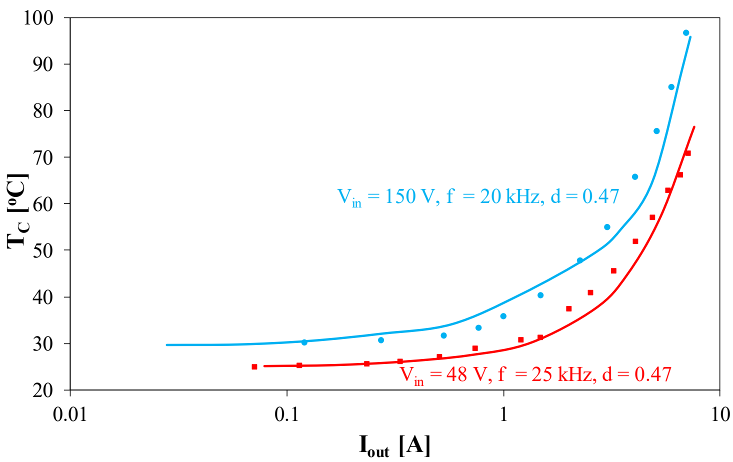

Figure 17. Computed and measured dependences of the module temperature on the output current of the half-bridge converter.

In all these figures, the results of measurements fit very well the computations results. In Figure 15, it is visible that an increase in the input voltage causes nearly a proportional increase in the output voltage. Additionally, an increase in the output current causes a decrease in the converter output voltage. Discrepancies between the computations and measurements results visible at V_{in} = 150 V can be observed due to the fact that thermal phenomena in diodes D_3 and D_4 and non-linearities of the characteristics of magnetic components are omitted.

Only the average values of the output voltage, the case temperature, and the dissipated power are presented for the steady state. Of course, in the computations, we observed the ripples in the waveforms of voltage, currents, and junction temperatures, but the peak-to-peak values of these ripples are much lower than the average values of the mentioned quantities. For example, the ripples in the output voltage have the peak-to-peak value not exceeding 40 mV.

A very important parameter of DC-DC converters is energy efficiency η. The value of this parameter is limited by, e.g., power losses in semiconductor devices [39,40]. Such losses depend on the junction temperature of the mentioned devices; therefore, thermal phenomena influence energy efficiency. The dependences $\eta(I_{out})$ shown in Figure 16 possess a maximum, which shifts right when the input voltage increases. The same values of the output current of energy efficiency η are obtained at higher values of the input voltage. Differences in the values of η obtained at both the values of V_{in} exceed even 20%. These differences are the result of the fact that power losses in semiconductor devices do not visibly change with an increase in the converter input voltage, whereas the output power increases nearly proportionally to this voltage.

In Figure 17, it is visible that the case temperature of the module is an increasing function of the converter output current and the input voltage. This increase in T_C limits the range of the allowable output current at the fixed values of V_{in}, f, and d of the control signal. The accuracy of the performed analyses can be improved if dynamic properties of IGBTs and diodes that are important when switching these devices and considered, e.g., in [41,42] are taken into account.

4. Influence of Thermal Model Form on the Computations Results

In order to show an influence of the used form of the thermal model of the IGBT module on the accuracy of the computations of the components characteristics of this module, some analyses were performed. Some of the obtained results are shown in this section.

Four forms of the module thermal model were considered. In the first one (model A), no thermal phenomena are taken into account and the junction temperature of each component and the case temperature are equal to the ambient temperature. The computations results obtained using this model are denoted with black dashed lines. The second thermal model (model B) takes into account self-heating in each component only, whereas mutual thermal couplings are omitted. In this model, it is assumed that the thermal resistance is constant and it does not depend on the dissipated power. The results obtained using this model are denoted with blue lines. The third model (model C) takes into account both self-heating in each component and mutual thermal couplings between each pair of the components, but the values of self and transfer thermal resistances do not depend on the dissipated power. The results obtained using such a model are denoted with green lines. Finally, the nonlinear thermal model proposed in this article (model D) takes into account self-heating, mutual thermal couplings, and the dependence of self and transfer thermal resistances on the dissipated power. The results of the computations performed with this model are denoted with red lines.

In Figure 18a, the output characteristics of transistor T_1 at voltage V_{GE1} = 6.6 V are shown for the module operating without any heat-sink, whereas Figure 18b corresponds to the dependences of the case temperature on the collector-emitter voltage of transistor

T_1. The investigations were performed at different values of the power p_{T2} dissipated in transistor T_2.

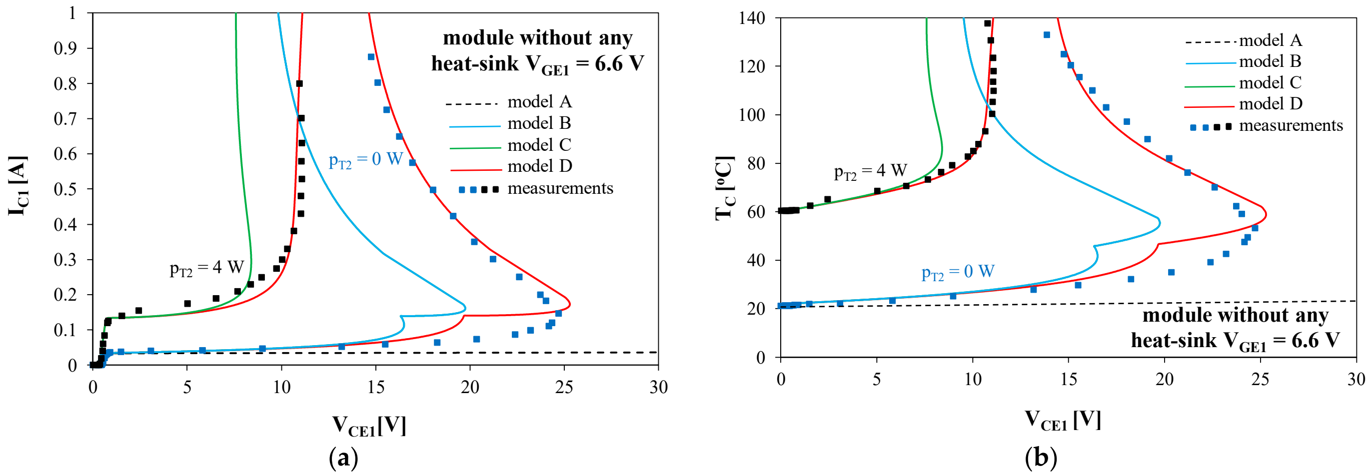

Figure 18. Output characteristics of transistor T_1 (**a**) and dependences of temperature T_C on voltage v_{CE1} (**b**) for the module operating without any heat-sink obtained using the measurements and computations with different thermal models.

As it is visible, only model D makes it possible to obtain a very good agreement between the results of computations and measurements for different values of the power dissipated in the other components of the tested module in a wide range of voltage and current. Model C allows one to obtain a satisfactory agreement between the measurement and computation results only at low values of the power dissipated in transistor T_1. An increase in this power causes wider discrepancies between the computations and measurements results due to a decreasing function of thermal resistance on the dissipated power, which is neglected in this model. For high values of current i_{C1}, voltage v_{CE1} is lowered even by 30%, and temperature T_C is overestimated by up to 30 °C. In turn, model B omits the influence of the power dissipated in transistor T_2 on the characteristics of transistor T_1 and has the same course for both the values of power p_{T2}. Therefore, for power $p_{T2} > 0$, the computed and measured characteristics differ significantly from each other. The computed values of the collector current i_{C1} are underestimated even up to 13 times, and temperature T_C is underestimated by over 100 °C. Model A makes it possible to obtain the acceptable accuracy of computations only at very low values of the dissipated power.

Figure 19 shows the output characteristics and the dependence $T_C(V_{CE1})$ for the module placed on the heat-sink.

The characteristics presented in Figure 19 show the advantage of model D over the other models under consideration. The quantitative differences between the results of computations and measurements with the considered models are on a similar level as for a transistor operating without any heat-sink. The differences between the results of measurements and the results of computations performed using models A, B, and C increase with an increase in the value of the power dissipated in the other components of the tested module.

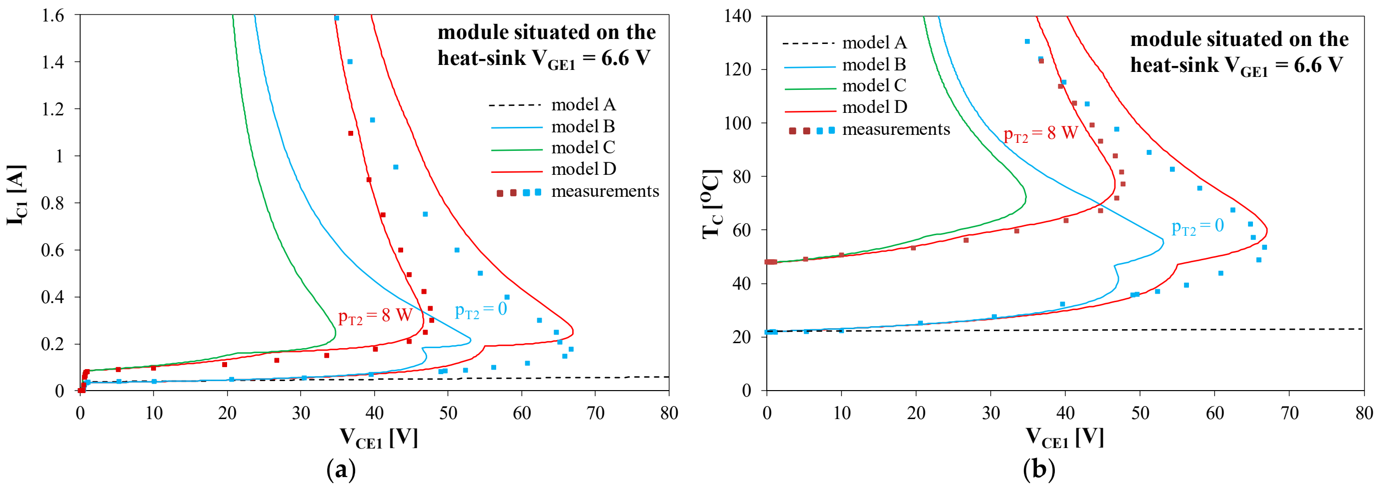

Figure 19. Output characteristics of transistor T_1 (**a**) and dependences of temperature T_C on voltage v_{CE1} (**b**) for the module situated on the heat-sink obtained using the measurements and computations with different thermal models.

5. Conclusions

The paper presents a large-signal electrothermal model of the IGBT module. This model is dedicated to SPICE and enables the determination of DC and dynamic characteristics of this module components and of the systems containing this module. It takes into account significant electrical phenomena occurring in transistors and diodes as well as thermal phenomena occurring in the module. These phenomena include self-heating in each component of the module and mutual thermal couplings between each pair of these components. Additionally, the non-linearities of the aforementioned thermal phenomena, characterized by their self and transfer thermal resistances depending on the power dissipated in the module, are taken into account.

The correctness of the proposed model was verified experimentally. The investigations were performed for the module of the type PSI25/06 by Power Sem operating at different cooling conditions. For all the considered cooling and operating conditions of this module, the results of computations fit well the results of the measurements. Due to the dependence of thermal resistances on the power, a much better accuracy in modeling the characteristics of the module components was achieved than with the model described in [34].

Table 2 compares the properties of selected models which make it possible to compute characteristics of the power modules.

Table 2. Properties of selected models used to compute the characteristics of power modules.

Source	Taking into Account:					
	Ambient Temperature	**Self-Heating**	**Mutual Thermal Couplings**	**R_{th}(p) or R_{th}(T)**	**Thermal Inertia**	**Sub-Threshold Effect**
[12]	YES	YES	NO	NO	YES	NO
[31]	YES	YES	YES	YES	YES	NO
[34]	YES	YES	YES	NO	YES	YES
This article	YES	YES	YES	YES	YES	YES

As can be easily observed, this article includes all the important phenomena taken into account in the previously published articles. On the other hand, it also takes into account the influence of the ambient temperature, self-heating, mutual thermal couplings, the dependence of thermal resistance on the dissipated power, and the sub-threshold effect in the IGBT.

The presented computation and measurement results showed that both the ambient temperature and thermal phenomena strongly influence the DC characteristics of the components of the tested IGBT module. An increase in the ambient temperature cause only quantitative changes in these characteristics, whereas thermal phenomena cause changes in the shape of the characteristics of the diode and the transistor situated in the IGBT module. For a low value of V_{GE} voltage, nearing the value of the threshold voltage on the transistor output characteristics, points of the electrothermal breakdown can be observed. Self-heating phenomena and mutual thermal couplings can cause a significant rise of the junction temperature of the module. Due to this rise, the value of the admissible power is visibly limited. The proposed model makes it also possible to accurately calculate the junction temperature of each component of the tested module.

The presented results of the analyses and measurements of the characteristics of the half-bridge converter proved that the proposed model enables the correct determination of its electrical characteristics, energy efficiency, and temperature of the module components. The obtained results confirmed that with a higher value of the input voltage of the converter, a much higher energy efficiency rating can be obtained. For example, changing the value of this voltage from 48 to 150 V allows for an increase in the maximum value of the efficiency from 80 to 90%. It can also be seen that an increase in this voltage also results in an increase in the junction temperature of the module components caused by an increase in the power loss associated with switching on or off the transistors contained in the module.

The presented model and test results may be useful for designers of systems which contain power modules. Changes in the component characteristics of such modules can be similarly modeled for modules containing other semiconductor devices, e.g., power MOSFETs.

Author Contributions: Conceptualization: K.G. and P.G.; methodology: K.G. and P.G.; investigation: K.G. and P.G.; writing—original draft preparation: K.G. and P.G.; writing—review and editing: K.G. and P.G.; visualization: K.G. and P.G.; supervision: K.G. All authors have read and agreed to the published version of the manuscript.

Funding: The scientific work financed with the Polish science budget resources in the years 2017–2021, as the investigation project within the framework of the program "Diamentowy Grant" project No. DI2015 007545.

Data Availability Statement: Data is contained within the article.

Conflicts of Interest: The authors declare no conflict of interest.

References

1. Perret, R. *Power Electronics Semiconductor Devices*; John Wiley & Sons, Ltd.: Hoboken, NJ, USA, 2009.
2. Rashid, M.H. *Power Electronic Handbook*; Academic Press: Cambridge, MA, USA; Elsevier: Amsterdam, The Netherlands, 2007.
3. Kazimierczuk, M.K. *Pulse-Width Modulated DC-DC Power Converters*; John Wiley &Sons, Ltd.: Hoboken, NJ, USA, 2008.
4. Lai, W.; Zhao, Y.; Chen, M.; Wang, Y.; Ding, X.; Xu, S.; Pan, L. Condition Monitoring in a Power Module Using On-State Resistance and Case Temperature. *IEEE Access* **2018**, *6*, 67108–67117. [CrossRef]
5. Stella, F.; Pellegrino, G.; Armando, E.; Dapra, D. Online Junction Temperature Estimation of SiC Power MOSFETS Through On-State Voltage Mapping. *IEEE Trans. Ind. Appl.* **2018**, *54*, 3453–3462. [CrossRef]
6. Dbeiss, M.; Avenas, Y.; Zara, H. Comparison of the electro-thermal constrains on SiC MOSFET and Si IGBT power modules in photovoltaic DC/AC inverters. *Microelectron. Reliab.* **2017**, *78*, 65–71. [CrossRef]
7. Mitsubishi Electronics Corporation. *Mitsubishi Semiconductors Power Module MOS—Data Book*; Mitsubishi Electronics Corporation: Tokyo, Japan, 1995.
8. An, N.; Du, M.; Hu, Z.; Wie, K. A High-Precision Adaptive Thermal Network Model for Monitoring of Temperature Variations in Insulated Gate Bipolar Transistor (IGBT) Modules. *Energies* **2018**, *11*, 595. [CrossRef]
9. Bahman, A.; Ma, K.; Blaabjerg, F. A lumped Thermal Model Including Thermal Coupling and Thermal Boundary Conditions for High-Power IGBT Modules. *IEEE Trans. Power Electron.* **2018**, *33*, 2518–2530. [CrossRef]
10. Castellazzi, A.; Kraus, R.; Seliger, N.; Schmitt-Landsiedel, D. Reliability analysis of power MOSFET's with the help of compact models and circuit simulation. *Microel. Reliab.* **2002**, *42*, 1605–1610. [CrossRef]
11. Bryant, A.T.; Mawby, P.A.; Palmer, P.R.; Santi, E.; Hudgins, J.L. Exploration of power device reliability using compact device models and fast electrothermal simulation. *IEEE Trans. Ind. Appl.* **2008**, *44*, 894–903. [CrossRef]

12. Hefner, A.R.; Diebolt, D.M. An Experimentaly Verified IGBT Model Implemented in the Saber Circuit Simulator. *IEEE Trans. Power Electron.* **1994**, *9*, 532–542. [CrossRef]
13. Mawby, P.A.; Igic, P.M.; Towers, M.S. Physically based compact device models for circuit modelling applications. *Microelectron. J.* **2001**, *32*, 433–447. [CrossRef]
14. Starzak, Ł.; Zubert, M.; Janicki, M.; Torzewicz, T.; Napieralska, M.; Jabłoński, G.; Napieralski, A. Behavioral approach to SiC MPS diode electrothermal model generation. *IEEE Trans. Electron. Devices* **2013**, *60*, 630–638. [CrossRef]
15. Górecki, P.; Górecki, K.; Zarębski, J. Accurate circuit-level modelling of IGBTs with thermal phenomena taken into account. *Energies* **2021**, *14*, 2372. [CrossRef]
16. Lasance, C.J.M.; Poppe, A. *Thermal Management for LED Applications*; Springer Science Business Media: New York, NY, USA, 2014.
17. Górecki, K.; Ptak, P. Compact modelling of electrical, optical and thermal properties of multi-colour power LEDs operating on a common PCB. *Energies* **2021**, *14*, 1286. [CrossRef]
18. Scognamillo, C.; Fregonese, S.; Zimmer, T.; d'Alessandro, V.; Catalano, A.P. A Technique for the In-Situ Experimental Extraction of the Thermal Impedance of Power Devices. *IEEE Trans. Power Electron.* **2022**, *37*, 11511–11515. [CrossRef]
19. D'Alessandro, V.; Codecasa, L.; Catalano, A.P.; Scognamillo, C. Circuit-based electrothermal simulation of multicellular sic power MOSFETs using FANTASTIC. *Energies* **2020**, *13*, 4563. [CrossRef]
20. Azar, R.; Udrea, F.; Ng, W.T.; Dawson, F.; Findlay, W.; Waind, P.; Amaratunga, G. Advanced electrothermal Spice modelling of large power IGBTs. *IEE Proc. Circuits Devices Syst.* **2004**, *151*, 249–253. [CrossRef]
21. Górecki, P.; Górecki, K. Modelling a Switching Process of IGBTs with Influence of Temperature Taken into Account. *Energies* **2019**, *12*, 1894. [CrossRef]
22. Rashid, M.H.; Rashid, H.M. *Spice for Power Electronics and Electric Power*; CRC Press: Boca Raton, FL, USA, 2006.
23. Castellazzi, A. Comprehensive compact models for the circuit simulation of multichip power modules. *IEEE Trans. Power Electron.* **2010**, *25*, 1251–1264. [CrossRef]
24. Bouguezzi, S.; Ayadi, M.; Ghariani, M. Developing a Simplified Analitical Thermal Model of Multi-chip Power Module. *Microelectron. Reliab.* **2016**, *66*, 64–77. [CrossRef]
25. Wu, R.; Wang, H.; Pedersen, K.B.; Ma, K.; Ghimire, P.; Iannuzzo, F.; Blaabjerg, F. A temperature-dependent thermal model of IGBT modules suitable for circuit-level simulations. *IEEE Trans. Ind. Appl.* **2016**, *52*, 3306–3314. [CrossRef]
26. Zhang, Y.; Wang, H.; Wang, Z.; Yang, Y.; Blaabjerg, F. Simplified Thermal Modeling for IGBT Modules with Periodic Power Loss Profiles in Modular Multilevel Converters. *IEEE Trans. Ind. Electron.* **2019**, *66*, 2323–2332. [CrossRef]
27. Chang, Y.; Li, W.H.; Luo, H.Z.; He, X.N.; Iannuzzo, F.; Blaabjerg, F.; Lin, W.X. A 3D Thermal Network Model for Monitoring Imbalanced Thermal Distribution of Press-Pack IGBT Modules in MMC-HVDC Applications. *Energies* **2019**, *12*, 1319. [CrossRef]
28. Luo, Z.H.; Ahn, H.; El Nokali, M.A. A thermal model for insulated gate bipolar transistor module. *IEEE Trans. Power Electron.* **2004**, *19*, 902–907. [CrossRef]
29. Wang, J.; Chen, W.; Zhang, J.; Xu, M.; Wang, L.; Liu, J.; Gan, Y. A Novel Approach to Model and Analyze Uneven Temperature Distribution Among Multichip High-Power Modules and Corresponding Method to Respecify Device SOA. *IEEE Trans. Power Electron.* **2022**, *37*, 4626–4640. [CrossRef]
30. Reichl, J.; Ortiz-Rodriguez, J.M.; Hefner, A.; Lai, J.S. 3-D Thermal Component Model for Electrothermal Analysis of Multichip Power Modules with Experimental Validation. *IEEE Trans. Power Electron.* **2015**, *30*, 3300–3308. [CrossRef]
31. Van der Broeck, C.; Ruppert, L.A.; Hinz, A.; Conrad, M.; De Doncker, R.W. Spatial Electro-Thermal Modeling and Simulation of Power Electronic Modules. *IEEE Trans. Ind. Appl.* **2018**, *54*, 404–415. [CrossRef]
32. Nwanoro, K.C.; Lu, H.; Yin, C.; Bailey, C. Numerical simulation of the junction temperature, the coolant flow rate and the reliability of an IGBT module. In Proceedings of the 24th International Workshop on Thermal Investigations of ICs and Systems THERMINIC, Stockholm, Sweden, 26–28 September 2018; pp. 1–6.
33. Górecki, K.; Górecki, P.; Zarębski, J. Measurements of parameters of the thermal model of the IGBT module. *IEEE Trans. Instrum. Meas.* **2019**, *68*, 4864–4875. [CrossRef]
34. Górecki, P.; Górecki, K. Modelling dc characteristics of the IGBT module with thermal phenomena taken into account. In Proceedings of the 13th International Conference on Compatibility, Power Electronics and Power Engineering (CPE-POWERENG), Sonderborg, Denmark, 23–25 April 2019. [CrossRef]
35. Górecki, K.; Zarębski, J.; Górecki, P.; Ptak, P. Compact thermal models of semiconductor devices—A review. *Int. J. Electron. Telecommun.* **2019**, *65*, 151–158. [CrossRef]
36. PSI 25/06 Power Module, Data Sheet, PowerSem. Available online: https://www.powersem.net/IGBT_Modules/Ecoline/PSIG-PSI-PSSI-PSIS%2025-06.pdf (accessed on 7 November 2023).
37. IR2110(S)PbF/IR2113(S)PbF High and Low Side Driver, International Rectifier, Data Sheet No. PD60147 rev.V. Available online: https://www.infineon.com/dgdl/Infineon-IR2110-DataSheet-v01_00-EN.pdf?fileId=5546d462533600a4015355c80333167e (accessed on 7 November 2023).
38. Wilamowski, B.; Jager, R.C. *Computerized circuit Analysis Using SPICE Programs*; McGraw-Hill: New York, NY, USA, 1997.
39. Ericson, R.; Maksimovic, D. *Fundamentals of Power Electronics*; Kluwer Academic Publisher: Norwell, MA, USA, 2001.
40. Iqbal, M.T.; Maswood, A.I.; Tariq, M.; Iqbal, A.; Verma, V.; Urooj, S. A Detailed Full-Order Discrete-Time Modeling and Stability Prediction of the Single-Phase Dual Active Bridge DC-DC Converter. *IEEE Access* **2022**, *10*, 31868–31884. [CrossRef]

41. Bryant, A.T.; Lu, L.; Santi, E.; Hudgins, J.L.; Palmer, P.R. Modeling of IGBT Resistive and Inductive Turn-On Behavior. *IEEE Trans. Ind. Appl.* **2008**, *44*, 904–914. [CrossRef]
42. Jahdi, S.; Alatise, O.; Ran, L.; Mawby, P. Accurate Analytical Modeling for Switching Energy of PiN Diodes Reverse Recovery. *IEEE Trans. Ind. Electron.* **2015**, *62*, 1461–1470. [CrossRef]